A First-Order Noise Analysis of the GBT L-Band Receiver Front-End

Richard F. Bradley

January 30, 2003

Introduction

Recent investigations of GBT baselines associated with observations of continuum radio sources have revealed the presence of several frequency dependent anomalies in the spectra produced by traditional calibration and normalization practices [1, 2, 3]. The (sig - ref) / ref formulation, where "sig" is the signal produced at the receiver's output when the telescope is pointing on source and "ref" is the corresponding signal when the telescope is pointing off source, indicates overall large-scale frequency structure as well as periodic, small-scale frequency structure. These structures are present in the L-, C-, and X-band receivers that were evaluated during the commissioning process, and it may well be present at other bands. Through a series of tests performed by R. Fisher and R. Norrod, the cause of this spectral anomaly within the GBT instrumentation has been localized to being ahead of the first mixer in the receiver's RF component chain. It was agreed that first-order modeling and simulation of this cascaded microwave network was necessary to begin to understand the origin of this phenomenon so that corrective action can be taken.

L-band was chosen for the simulation since a well-understood equivalent circuit model is available for the low-noise amplifier used in this band. A block diagram of the RF front-end components of the L-band receiver are shown in Fig. 1. The RF components at a physical temperature of 300 K include the feed, interconnecting waveguide, dewar vacuum seal, and a section of the thermal gap. At 15 K, there is another section of the thermal gap, the ortho-mode transition (OMT), calibration coupler, and low noise amplifier. The system noise temperature of this receiver on the GBT was measured to be approximately 18.5 K. A rough estimate of the noise budget [4] assigns 5 K for atmosphere and CMBR, 5 K for spillover, 4-5 K for the feed, window, OMT, and coupler cascade, and 3-4 K for the low nosie amplifier. The feed length is about 3.3 meters [4] yielding a total electrical length from amplifier to the feed aperture of about 4 meters [4].

A typical composite Tsource / Tsys spectra from 1300-1500 MHz for a continuum radio source taken with the GBT [3] is shown in Fig. 2. These spectra are illustrative of the typical frequency structure encountered in GBT baselines. There is an overall slope across this band together with a sinusoidal-like variation. It is these structures that will be addressed with the simulation and modeling described here. In addition, the spectra shows some very small-scale structure that is believed to be caused by the telescope's optics [5] along with know negative-going interference spikes [5]. Both of these structures reside outside the scope of this study.

Noise Theory

In order to obtain a rough estimate of the various noise contributions within a microwave network, it is common practice to model the loss as merely a perfectly matched attenuator that generates noise proportional to its physical temperature, as described by equation. 7-55a on p. 291 of Kraus [6]. This approach yields a quantity that is actually the *minimum* equivalent noise temperature, Tmin, of the matched lossy component. Implicit in this model is the assumption that the noise waves emanating from the two ports of the attenuator are statistically independent. This is usually not the case in practice.

The complex two-port noise model, which is defined by four noise parameters, is a more complete model of the noise properties of an RF component [7, 8]. A derivation of this noise model is given in Appendix A, but it can be summarized as

$$T_n = T_{MIN} + \frac{T_{REF} G_n}{R_S} \left| Z_S - Z_{opt} \right|^2 , \qquad \textbf{(1)}$$

where Tmin is the minimum noise temperature of the network, Gn is the noise conductance, Zopt=Ropt+jXopt is the optimum noise impedance, and Zs = Rs+jXs is the impedance presented to the input of the attenuator. Tref = 290 K. This equation shows that the amount of noise power as a function of frequency that flows out of the output port of the lossy two-port network will depend on the *complex circuit impedance* that terminates the component's input port. Note that the second term is a positive going quadratic function of the difference between the input impedance and the optimum noise impedance. This function is centered about the optimum noise impedance.

Component Models

The approach adopted here for modeling the frequency behavior of the L-band front-end is to first develop a suitable equivalent circuit and noise model for each of the critical components in the RF signal path that are thought to be contributing to the varying baseline phenomenon. A circuit simulator, namely Agilent's Advanced Design System (ADS), was used to determine the RF network behavior and calculate (sig - ref) / ref in order to emulate GBT observations. Three critical network element have been identified: 1) basic circuit loss, 2) the cascade comprised of the feed, dewar waveguide transition, and OMT, and 3) the low noise amplifier. Details of each component are given below.

Basic Circuit Loss

The noisy elements within the network are assumed to be generated by discrete losses that can be modeled by a pi-type attenuator pad made from individual ADS resistor models. A careful study of the behavior of the overall circuit model under various conditions confirmed that it was indeed functioning as a complex two-port noise model. Two attenuators were chosen to illustrate the differences between the perfectly matched model and the full complex two-port noise model. In both cases, the attenuators were designed for 0.1 dB power loss using the hyperbolic formulae

given in [9] and are at a physical temperature of 300 K. Attenuator #1 was designed to perfectly match the embedding network impedance of 50 ohms. Attenuator #2 was designed for 100 ohms but used in the same 50 ohm embedding network as attenuator #1. This situation could represent a loss element whose optimum noise resistance differs significantly from the network impedance. The results of the ADS simulations are summarized in Table 1.

Table 1 ADS simulation results for the two attenuators described in the text.

Zatt [ohms]	|S21| [dB]	|S11| [dB]	Tn [K]	Tmin [K]	Ropt [ohms]	Xopt [ohms]	Gn [mS]
50	-0.099	-125	6.991	6.99	50	0	0.238
100	-0.125	-41	8.719	6.99	100	0	0.119

Note that if |S21| is used to predict the noise contribution we would calculate 6.92 K for attenuator #1 and 8.76 K for attenuator #2 which is quite close to Tn. However, we completely miss the fact that Tn is not equal to Tmin for attenuator #2. The extra 1.73 K is actually coming from the second term in Eqn. 1.

In order to gauge the effect of the second term in Eqn. 1, an ADS simulation was carried out on the two attenuators for the condition of a varying input impedance, with Rs ranging from 45 - 55 ohms and Xs ranging from -5 to +5 ohms. The results are plotted in Fig. 3. The noise temperature of both attenuators is a relatively weak function of the input reactance since both have Xopt = 0 ohms. The -5 to +5 ohms variation about the optimum reactance produced only a 0.5% or less increase in the noise temperature. However, the effect of varying the input resistance is more pronounced. For Attenuator #1, the ± 5 ohm variation around 50 ohms (which is also Ropt in this case) produced only a 0.5% increase in Tn above Tmin. On the other hand, Attenuator #2, whose optimum noise resistance is 100 ohms, produced a ± 6% variation in Tn about the value at 50 ohms.

Feed, dewar transition, and OMT cascade

Reflectrometry measurements of the feed, dewar transition, and OMT cascade were made by S. Srikanth [10] and are reproduced in Fig. 4. These measurements indicate reflections at the -25 to -30 dB level across the mid portion of the band. It was decided that a detailed model of this network was unnecessary at this time in favor of a simplified network consisting of a cascade of several 50 ohm transmission lines with small-value capacitors placed in shunt at each of the junction points, as illustrated in Fig. 5. The lines were modeled as lossless components so that a given amount of circuit loss could be inserted at various locations along the line to study the effects. AST was used to calculate the level and periodicity of these reflections as a function of shunt capacitance and line length. These parameters were adjusted until a first-order fit at mid-band was obtained between the model and the measured data. The calculated |S11| and terminal impedances are shown in Fig. 6

This lossless network was then placed ahead of the an attenuator as shown in Fig. 7. The attenuator was modeled as described in the previous section with both types being considered. A plot of the noise temperature versus frequency for the cascaded network is shown in Fig. 8. Note that in both cases the impedance variation presented to the input of the attenuator translates to noise temperature fluctuations for the attenuator. These fluctuation are much more pronounced for attenuator #2 (Zopt = 100 ohms) which is consistent with the noise model.

Low noise amplifier

The amplifier used in the GBT L-band receiver is a three-stage, single-ended design created by Gallego and Pospieszalski [11]. The three HFET's are type FHR02X that were manufactured by Fujitsu. An equivalent circuit model for the HFET is shown in Fig. 9. A block diagram of the amplifier is given in Fig. 10. Basic capacitor models were used in place of the more complete equivalent circuit models for the chip capacitors for this simulation. ADS was used to simulate the performance of this amplifier with input and output ports terminated in 50 + j0 ohms. The calculated S-parameters are shown in Fig. 11. Calculated noise parameters are given in Fig. 12.

The input impedance presented to the amplifier was systematically varied over the range $45 < Rin < 55$ ohms and $-5 < Xin < +5$ ohms and the noise temperature at 1.4 and 1.7 GHz was calculated. The results are presented in Fig. 13.

Front-End Configurations and Simulation Results

Several ADS simulations were performed to gain an understanding of the frequency structure observed in [Ton - Toff] / Toff for continuum radio sources. In all simulations, the characteristic impedance of the network was 50 ohms and an ADS two-port noise source model, perfectly matched to 50 ohms, was used to emulate a frequency independent antenna temperature for both on and off source conditions. Two identical networks, one with Ta(on) and one with Ta(off) were analyzed simultaneously so that the [Ton - Toff] / Toff could be easily calculated. Details of the individual simulations together with their results are presented below. Note that receiver gain drifts are not modeled here and that a perfectly stable receiver is assumed.

Large Scale, Non-Periodic Frequency Structure

The first simulation was designed to examine the origins of the large-scale frequency structure. It was hypothesized that this structure was a consequence of amplifier noise. The network, a block diagram of which is shown in Fig. 14, consisted of the antenna temperature noise source followed by the amplifier model. Ta(off) was 5 K while Ta(on) was varied from 0 - 10 K in steps of 2 K. The results are shown in Fig. 15. These data are presented graphically in two columns. The left hand column shows the on-source noise temperature T(on), off-source noise temperature T(off), [T(on) - T(off)], and [T(on) - T(off)] / T(off) for the network operating over the 1.0 - 2.0 GHz band. The right hand column shows the same sequence for a bandwidth of 40 MHz near 1.4 GHz.

These plots clearly show the frequency structure of the amplifier noise is carried through to the [T(on) - T(off)] / T(off) due to the use of this frequency dependent normalizing factor, T(off). Its

effect is a function of antenna temperature. In addition, the narrow band formulation indicates just how such broad band structure could have been easily hidden in past observations. This effect is not indicative of an inherent receiver problem, but a calibration and normalization issue that will affect observing technique. Note that receiver gain drifts are not modeled here and that a perfectly stable receiver is assumed.

Small Scale, Periodic Frequency Structure

The second simulation was designed to examine the origins of the small-scale, periodic frequency structure. The network consisted on the antenna temperature noise source, followed by the shunt capacitor loaded transmission lines, and the amplifier. Transmission line length Len2 was increased to 1000 cm to enhance the frequency variation for visualization purposes only. The results are presented in Fig. 16. The left hand column shows the on-source noise temperature T(on), off-source noise temperature T(off), [T(on) - T(off)], and [T(on) - T(off)] / T(off) for the network operating over the 1.3 - 1.5 GHz band. The right hand column shows on-source noise temperature T(on), off-source noise temperature T(off), and [T(on) - T(off)] / T(off) for the same network operating over a 40 MHz bandwidth near 1.4 GHz. In addition, |S11| for the transmission line section only is shown. Note that in this case, 9.5 K had to be included into Ta for both on and off source to make [T(on) - T(off)] / T(off) comply with GBT observations. In addition, the variation in [T(on) - T(off)] / T(off) is much smaller in amplitude than observed on the GBT but is in agreement with that expected from the amplifier due to impedance variation of the loaded transmission line. The amplitude variation is about the same if we make Len3=1000 cm and Len2=10 cm. These simulations suggest that although the variation in amplifier noise is certainly one component of the noise, there remains another noise mechanism that dominates.

A clue to the other mechanism comes from the 9.5 K needed to artificially raise the system temperature to that of the GBT L-band receiver. The previous simulation suggests that this noise is probably not due to spillover since this component would simply raise the overall noise temperature of the receiver without enhancing the variation we have observed on the GBT. Therefore, the extra noise was removed from Ta, modeled as an attenuator, and placed between the loaded transmission line and the amplifier. Two attenuators were investigated: one designed for Zopt = 50 ohms and the other with Zopt=150 ohms. The physical temperature of the attenuator was set to 300 K since an attenuator at a cryogenic temperature of 15 K would need to have an attenuation of over 2 dB to produce 9.5 K of noise, a situation that doesn't represent the loss measurements. The simulation results are given in Fig. 17 for an 0.1 dB, Zopt = 50 ohms attenuator (Len2 = 1000 cm) and Fig. 18 for an 0.06 dB, Zopt = 150 ohms attenuator (Len2 = 1000 cm). Fig. 19 shows the results for the 0.06 dB, Zopt = 150 ohms attenuator with Len2 = 135 cm. To first order, the results in Fig. 19 are in agreement with the GBT measurements presented in Fig. 2.

Conclusions

As a word of caution, the simulations results and conclusions based on them as presented in this report should be taken as pure speculation until they can be verified through careful experimentation either on the bench or via GBT observations. With that said, there are several conclusions that may be drawn from the simulations:

- The frequency structure observed in the (sig - ref) / ref is not present in (sig – ref) but occurs as a result of the frequency dependence inherent in the ref signal. This effect is not indicative of an inherent receiver problem, but a calibration and normalization issue that will affect observing technique for wide bandwidth applications.

- The large scale, non-periodic structure is probably due to the frequency dependent noise temperature of the low noise amplifier.

- The small-scale, periodic frequency structure is primarily due to noise generated by an ohmic loss at a physical temperature of 300 K located near the OMT end of the microwave network consisting of the feed and the vacuum window / thermal gap. This noise is effected by reflections at the -25 to -30 dB level within the structure. The simulations indicate that the optimum noise impedance for this source differs significantly from the waveguide impedance which causes noise fluctuations with frequency that are on the same scale as that of the found in the GBT baselines. Hence, this mechanism appears tho be the root cause for the frequency structure observed.

- The reflections that occur within the feed, dewar window, thermal gap, and OMT will cause frequency dependent variations in the noise temperature of the low noise amplifier. *However, the amplitude of these variations appear to be too small to account for the size of the variations observed in the GBT baselines.*

- Based on bench measurements and GBT baseline data, the reflections within the feed and vacuum window / thermal gap structure appear to be a result of two or more reflections, with one pair spaced about 135 cm apart.

- The use of an isolator or a balanced amplifier will not affect the primary source of the baseline structure. However, such devices will reduce the gain variations in the amplifier which are a direct result of the multiple reflections. Smoothing the gain variation with frequency should help to improve receiver stability by reducing the receiver's sensitivity to the physical characteristics of the front-end network.

References

[1] Fisher, J.R. “Sample of Baseline Stability of the 2-3 GHz GBT Receiver,” Project TAST_SB_02119, November 19, 2002, NRAO, Dec. 3, 2002.

[2] Fisher, J.R. “Second Baseline Test of the 2-3 GHz GBT Receiver,” Project TBASEJRF021202, December 2, 2002, NRAO, Dec. 3, 2002.

[3] Fisher, J.R. “Further Investigation of L-Band Baselines on Continuum Sources,” Project TBASEDSB021217, December 17, 2002, NRAO, Dec. 23, 2001.

[4] Norrod, R., Private Communication, Jan. 2003.

[5] Fisher, J. R. Private Communication, Jan. 2003.

[6] Kraus, J.D. Radio Astronomy, McGraw-Hill, New York, 1966, p. 291.

[7] Penfield P. and R. P. Rafuse, Varactor Applications, M.I.T. Press, Cambridge, MA. 1962, pp. 21 - 25.

[8] Collin, R. E. Foundations for Microwave Engineering, 2nd Ed. McGraw-Hill, New York, 1992, pp. 766-772.

[9] ITT , Reference Data for Radio Engineers, 6th Ed., Howard W. Sams, Indianapolis, IN, 1975, Ch. 11.

[10] Srikanth, S. Private Communication, Jan, 2003.

[11] Gallego, J. D. and M. W. Pospieszalski, “Design and Performance of Cryogenically-Coolable, Ultra Low-Noise, L-Band Amplifier,” NRAO Electronic Division Internal Report, No. 286, Mar. 1990.

Appendix A

Adopted from lecture notes - Bradley & Fisher, ASTR 535 Introduction to Radio Astronomy Instrumentation, University of Virginia, Spring 2001.

A.1 The Noise Temperature of a Two-Port Network as a Function of its Source Impedance

Consider the noisy two-port network having a complex source impedance, Z_S, at the input as shown in Fig. A.1a. Let's assume for the moment that this impedance has no noise associated with it. Fig. A.1b shows the same network with all of the noise generated within the network represented by its equivalent noise temperature, T_N , which is now associated with the source impedance, Z_S. There is a value of Z_S which minimizes the total noise out of a two-port network. We refer to this optimum value of Z_S as Z_{opt}.

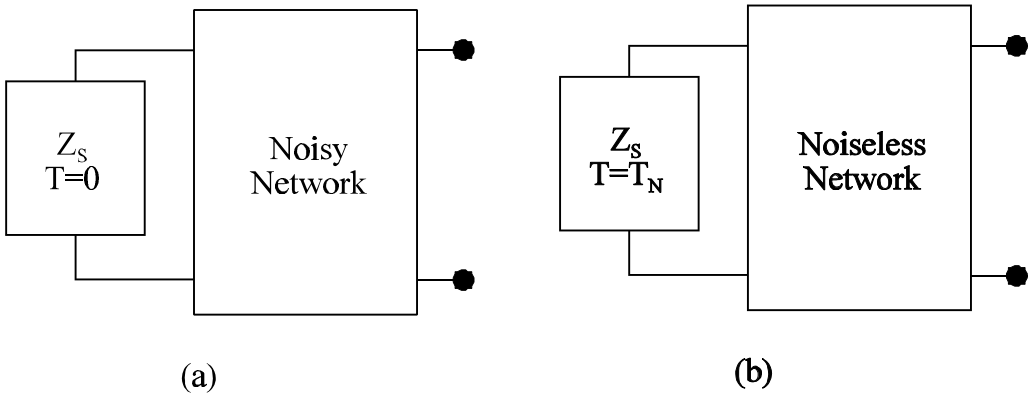

Figure A.1 Noisy network with source impedance Z_S (a) Noisy network. (b) Equivalent noise temperature representation.

Let us compute T_N and Z_{opt} in terms of the parameters of an *equivalent noise model* for the network. We choose the *Rothe-Dahlke Noise Model*, which represents the network of Fig. A.1 by the equivalent circuit shown in Fig. A.2a. This circuit consists of two noise sources: a voltage source, v_n , and a current source, i_n .

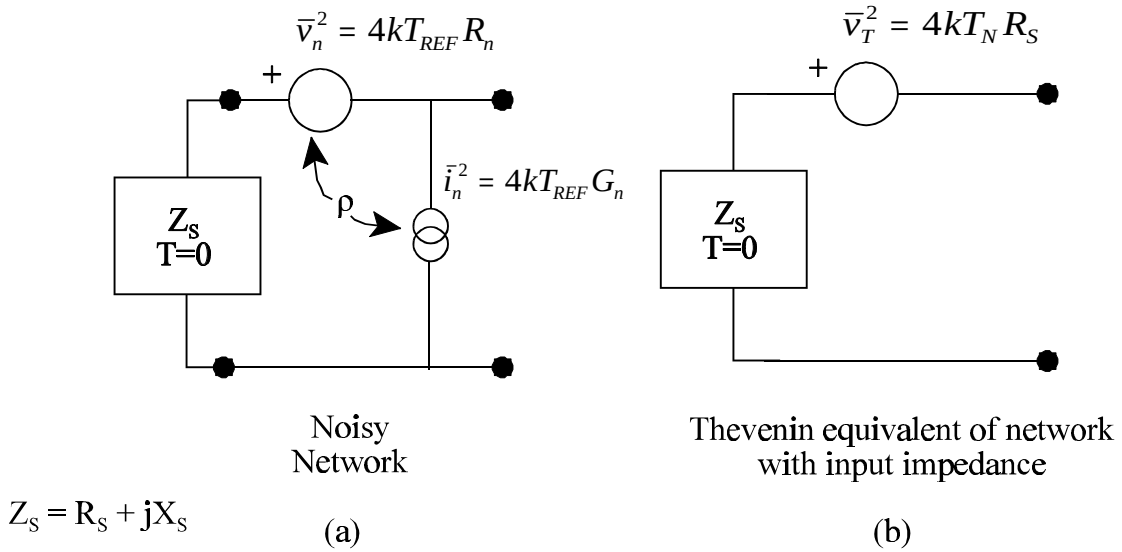

Figure A.2 (a) Noise model of network. (b) Thevenin equivalent circuit.

Two parameters, a resistance and a conductance, associated with these sources may be defined as

$$R_n = \frac{\bar{v}_n^2}{4kT_{REF}} \qquad \textbf{(A.1)}$$

and

$$G_n = \frac{\bar{i}_n^2}{4kT_{REF}}, \qquad \textbf{(A.2)}$$

where T_{REF} = 290 K.

We can treat the noise sources as random variables, and recall that the variance of a random variable is

$$Var[X] = \mathsf{E}[(X - m_X)^2] = \int_{-\infty}^{+\infty} (x - m_X)^2 f_X(x)dx\,. \qquad \textbf{(A.3)}$$

Similarly, we can define the *covariance* of two random variables, in this case v_n and i_n, as

$$\mathrm{cov}[v_n, i_n] = \mathsf{E}\left[(v_n - m_{v_n})(i_n - m_{i_n})\right] \qquad \textbf{(A.4)}$$

Since we can interchange the expected value and summation, and noting that our random variables have zero mean, we can expand Eq. A.4 as

$$\begin{aligned} \mathsf{E}\left[(v_n - m_{v_n})(i_n - m_{i_n})\right] &= \mathsf{E}\left[v_n i_n\right] - m_{v_n}\mathsf{E}\left[i_n\right] - m_{i_n}\mathsf{E}\left[v_n\right] + m_{v_n} m_{i_n} \ , \\ \mathrm{cov}[v_n, i_n] &= \mathsf{E}\left[v_n i_n\right] . \end{aligned} \tag{A.5}$$

Given two random variables, the ratio of the covariance to the product of the standard deviations is the *correlation coefficient, ñ,* such that

$$r = \frac{\mathrm{cov}\left[v_n, i_n\right]}{s_{v_n} s_{i_n}} = \frac{\mathsf{E}\left[v_n i_n\right]}{\sqrt{\mathsf{E}\left[v_n^2\right]\mathsf{E}\left[i_n^2\right]}} , \tag{A.6}$$

where we have made use of the fact that both v_n and i_n have zero mean. Note that the correlation coefficient is complex: $\tilde{n} = \tilde{n}_R + j\tilde{n}_I$.

The objective of the calculations that follow is to find T_n as a function of R_n, G_n, $\tilde{n}$, and Z_S that gives identical mean square voltage from both equivalent circuits,

$$\overline{v}_T^2 = \left(v_n + i_n Z_S\right)^2 = \left|\overline{v}_n\right|^2 + \left|\overline{i}_n\right|^2 \left|\overline{Z}_S\right|^2 + 2\,\mathrm{Re}\left\{i_n v_n Z_S\right\} . \tag{A.7}$$

We now substitute the expressions for the voltage and current into Eq. A.7 and solve for T_n / T_{REF} giving

$$\frac{T_n}{T_{REF}} = \frac{R_n}{R_S} + \frac{G_n}{R_S}\left(R_S^2 + X_S^2\right) + \frac{2\sqrt{R_n G_n}}{R_S}\left[r_R R_S - r_I X_S\right] . \tag{A.8}$$

The function $T_n / T_{REF}\,(R_S, X_S)$ is real-valued and the minimum point on the surface defined by this function can be found by setting the gradient equal to zero,

$$\nabla \frac{T_n}{T_{REF}}(R_S, X_S) = \left[\frac{\partial\, T_n/T_{REF}\,(R_S, X_S)}{\partial\, R_S}, \frac{\partial\, T_n/T_{REF}\,(R_S, X_S)}{\partial\, X_S}\right] = \vec{0} . \tag{A.9}$$

First, we begin by taking the partial derivative of Eq. A.8 with respect to X_S giving

$$\frac{\partial\, T_n/T_{REF}\,(R_S, X_S)}{\partial\, X_S} = \frac{2G_n X_S}{R_S} - \frac{2\sqrt{R_n G_n}\, r_I}{R_S} = 0 . \tag{A.10}$$

Solving for $X_S = X_{opt}$ yielding the equation for X_{opt} as

$$X_{opt} = \sqrt{\frac{R_n}{G_n}} r_I \ . \qquad \textbf{(A.11)}$$

Next, we take the partial derivative of Eq. A.8 with respect to R_S giving

$$\frac{\partial \, T_n / T_{REF} \, (R_S, X_S)}{\partial \, R_S} = -\frac{R_n}{R_S^2} + G_n - \frac{G_n X_S^2}{R_S^2} + \frac{2\sqrt{R_n G_n}\, r_I X_S}{R_S^2} = 0 \qquad \textbf{(A.12)}$$

Solving for $R_S^2 = R_{opt}^2$ gives

$$R_{opt}^2 = \frac{R_n}{G_n} + X_S^2 - 2\sqrt{\frac{R_n}{G_n}} r_I X_S \ . \qquad \textbf{(A.13)}$$

Substituting $X_S = X_{opt}$ from Eq. A.11 gives

$$R_{opt}^2 = \frac{R_n}{G_n}\left[1 - r_I^2\right]. \qquad \textbf{(A.14)}$$

We can now determine Z_{opt} from Eqs. A.14 and A.11 as

$$\left|Z_{opt}\right|^2 = \left|R_{opt}\right|^2 + \left|X_{opt}\right|^2 = \frac{R_n}{G_n}\left[1 - r_I^2\right] + \frac{R_n}{G_n} r_I^2 \ ,$$
$$\left|Z_{opt}\right|^2 = \frac{R_n}{G_n} \ . \qquad \textbf{(A.15)}$$

The minimum noise temperature, T_{min}, can be found by substituting R_{opt} and X_{opt} into Eq. A8 giving

$$\frac{T_{MIN}}{T_{REF}} = \frac{R_n}{R_{opt}} + \frac{G_n}{R_{opt}}(R_{opt}^2 + X_{opt}^2) + \frac{2\sqrt{R_n G_n}}{R_{opt}}(r_R R_{opt} - r_I X_{opt}) \ . \qquad \textbf{(A.16)}$$

With a little algebra we can simplify this equation to the following form:

$$T_{MIN} = 2\sqrt{R_n G_n}\left[\sqrt{1 - r_I^2} + r_R\right]T_{REF} \ . \qquad \textbf{(A.17)}$$

Since the function T_n (Z_S) is analytic around the minimum, we can find a compact expression for T_n near T_{MIN} by Taylor series expansion of T_n about the point T_{MIN},

$$\begin{aligned} T_n(Z_S) = {} & T_n(Z_S)\Big|_{Z_S = Z_{opt}} \\ & + \frac{dT_n(Z_S)}{dZ_S}\Bigg|_{Z_S = Z_{opt}} \left|Z_S - Z_{opt}\right| \\ & + \tfrac{1}{2}\frac{d^2T_n(Z_S)}{dZ_S}\Bigg|_{Z_S = Z_{opt}} \left|Z_S - Z_{opt}\right|^2 . \end{aligned} \qquad \textbf{(A.18)}$$

The first term is simply T_{MIN} . The second term is zero since the expansion is about the minimum point. The third term yields,

$$\begin{aligned} \frac{dT_n(Z_S)}{d(Z_S)} &= \frac{2T_{REF}G_n|Z_S|}{R_S} + \frac{2\sqrt{G_n R_n}T_{REF}\,r_R}{R_S}, \\ \frac{d^2T_n(Z_S)}{dZ_S^2} &= \frac{2T_{REF}G_n}{R_S}, \\ \therefore\ \tfrac{1}{2}\frac{d^2T_n(Z_S)}{dZ_S^2}\Bigg|_{Z_S = Z_{opt}} \left|Z_S - Z_{opt}\right|^2 &= \frac{T_{REF}G_n}{R_S}\left|Z_S - Z_{opt}\right|^2 , \end{aligned} \qquad \textbf{(A.19)}$$

or

$$T_n = T_{MIN} + \frac{T_{REF}G_n}{R_S}\left|Z_S - Z_{opt}\right|^2 . \qquad \textbf{(A.20)}$$

If we define the parameter $N = G_n R_{opt}$ then,

$$T_n = T_{MIN} + \frac{NT_{REF}\left|Z_S - Z_{opt}\right|^2}{R_S R_{opt}} . \qquad \textbf{(A.21)}$$

There are a couple of important points to make regarding Eq. A.21. We can now define four parameters associated which the noise generated within any two-port network: T_{MIN}, R_{opt}, X_{opt}, and N. When the source impedance is equal to the optimum noise impedance, the noise temperature of the network is equal to the minimum noise temperature, T_{MIN}. However, if there is a mismatch between Z_S and Z_{opt}, then the noise temperature will always be higher then T_{MIN} and related to the square of the difference between these impedances.